Table 1 Clinical findings and *PTPN11* mutations in our Noonan syndrome (NS) patients. *ASD* atrial septal defect, *PDA* patent ductus arteriosus, *PS* pulmonary stenosis, *VSD* ventricular septal defect, *PR* pulmonary valve regurgitation, *?* unknown, *JMML* juvenile myelomonocytic leukemia, *NB* neuroblastoma, *TAM* transient abnormal myelopoiesis, *N-SH2* aminoterminal SH2, *C-SH2* carboxyl terminal SH2, *PTP* protein tyrosine phosphatase

Patient	1	2	3	4	5	6	7	8	9	10	11	12	13	14	15	16
Gender	M	M	M	F	F	M	F	F	F	M	M	M	M	F	M	F
Age	12 years	6 years	14 years	1 years 9 Months	2 years	9 Months	11 years	19 years	8 years	22 years	3 years	14 years	7 years	12 Months	8years	3 years
Short stature (Standard deviation)	+	+ (−3.2)	+ (−2.5)	+	− (−2.0)	− (−1.6)	+	+	− (−1.1)	− (−1.6)	− (−1.6)	+ (−2.5)	+ (−3.3)	+ (−2.4)	− (−1.5)	− (−1.8)
Facial anomalies																
Hypertelorism	+	+	+	+	+	+	+	−	+	+	+	+	+	+	+	+
Ptosis	+	−	+	−	−	+	−	+	−	−	−	+	?	−	−	−
Down-slanting parpebral fissures	+	+	−	+	+	+	+	−	+	−	−	+	+	+	+	+
Low-set ears	−	+	−	+	−	+	+	−	+	−	−	−	+	+	−	+
Webbed neck	+	+	+	+	−	+	+	−	+	−	+	+	?	+	+	−
Cubitus valgus	+	−	+	+	+	−	+	−	+	−	+	+	?	+	+	−
Cardiovascular anomalies	ASD	−	−	PDA	PS ASD	ASD	PS ASD	−	PS	PS	PS	PS	PS ASD	PS ASD VSD	PS PR	PS ASD HCM
Cryptorchidism	?	−	+	−	−	Hydrocele	−	−	−	+	+	−	−	−	−	−
Mental retardation	−	−	−	+	−	+	+	+	−	−	+	−	−	−	−	+
Miscellaneous	Bleeding diathesis					Familial	Bleeding diathesis	JMML leuko-cytosis					Macro-cephaly	NB TAM	Skin pigmentation Hydrocephalus	Large tongue
PTPN11 mutation																
Exon	3	3	3	3	3	3	3	3	3	3	7	7	8	13	13	13
Nucleotide substitution	181G > A	181G > A	188A > G	188A > G	188A > G	211T > A	218T > C	218T > C	236A > G	236A > G	844A > G	844A > G	922A > G	1504T > A	1510A > G	1510 A > G
Amino acid substitution	D61N	D61N	Y63C	Y63C	Y63C	F71I	T73I	T73I	Q79R	Q79R	I282V	I282V	N308D	S502T	M504V	M504V
Domain	N-SH2	N-SH2	N-SH2	N-SH2	N-SH2	N-SH2	N-SH2	N-SH2	N-SH2	N-SH2	PTP	PTP	PTP	PTP	PTP	PTP

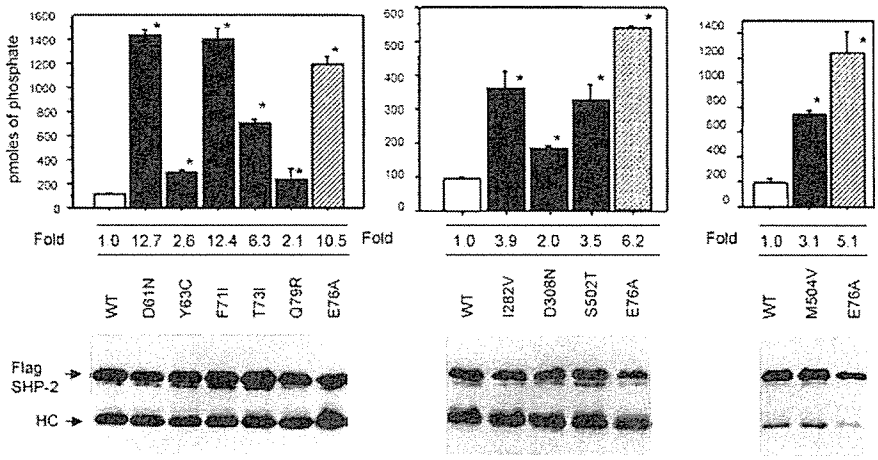

Fig. 1 Immune complex phosphatase assay of wild-type (WT) cDNA and mutants identified in Noonan syndrome (NS). The E76A mutant was used as a positive control in each assay. Results are expressed as mean ± SD obtained from three independent experiments. *Asterisks* indicate statistically significant differences ($p < 0.01$) in activity compared with that of WT. Fold activation was expressed as 1 for WT cDNA at each assay (*upper panel*). Immunoblot analysis of *SHP-2* showed the comparative efficiency of immunoprecipitation (*lower panel*). *HC* heavy chain

rapidly. These results suggest that these two mutants do not promote the activation of the MAPK pathway in EGF-treated 293 cells.

In order to examine the downstream signaling pathway of ERK, we examined the activation of the serum-responsive element (SRE) within c-fos or other immediate early genes in EGF-treated 293 cells. As a key target of MAPK, ELK1 transcription factors phosphorylated by ERK bind to the SRE to initiate transcription (Bennett et al. 1996; Hakak and Martin 1999). Cells expressing the SRE-luciferase reporter gene and a catalytically inactive SHP-2 (C459S) showed a decreased induction of the luciferase gene in the presence of EGF (Fig.2b). Cotransfection of plasmids harboring mutants detected in NS had neither enhanced SRE activity in the unstimulated state nor enhanced fold induction in the presence of EGF. These results suggest that the SHP-2 mutants did not promote the MAPK pathway in the EGF-treated 293 cells whereas they showed enhanced phosphatase activity in vitro.

Discussion

In this study, we identified nine mutations, including a novel F71I mutation, in 16 of 41 Japanese patients with NS and two mutations, including a novel G503V mutation, in three of 29 patients with childhood leukemia. Immune complex phosphatase assays showed that the phosphatase activity in ten SHP-2 mutants detected in NS and four SHP-2 mutants detected in leukemia was elevated to various degrees. Mutations in the *PTPN11* gene were detected in 39% of the patients clinically diagnosed with NS. This result is comparable to that of previous studies (Tartaglia et al. 2002; Musante et al. 2003). Previous genotype–phenotype correlation studies have shown that pulmonary stenosis was associated with *PTPN11* mutations whereas cardiomyopathy was more common in patients without *PTPN11* mutation (Tartaglia et al. 2002; Zenker et al. 2004). In our study, however, no significant difference was observed (data not shown). Although other abnormalities than exonic mutations in *PTPN11* have not been excluded, further studies to identify the gene(s) associated with NS will pose a formidable challenge in establishing the clinical entity of NS.

The role of *PTPN11* mutations in the pathogenesis of hematologic malignancy remains to be elucidated. In the previous and the present studies, 87% of the mutations found in leukemia cells were identified in the N-SH2 domain, and these were primarily restricted to residues D61, A72, and E76 (Tartaglia et al. 2003; Loh et al. 2004; Tartaglia et al. 2004). To examine whether the degrees of phosphatase activity in mutations at specific residues are associated with leukemia, we compared the phosphatase activity at each affected residue examined in this study, as well as the published phenotype (Table 2a). Variation of each assay was normalized as relative phosphatase activity; activity of WT cDNA was taken as one-fold, and that of E76A was taken as ten-fold. Mutations at codons 61, 71, 72, and 76, in which highest activity at each codon was ten or more, were frequently identified in patients with leukemia, including those with JMML, MDS, AML, and ALL (Table 2a). In NS patients, activities of the most common mutations at N308 and Y63 were two-fold to three-fold. The phosphatase activity of the T73I mutation, which is frequently detected in NS patients associated with JMML, showed an intermediate value of 6.0. Mutations at residues in which activities were below six were rarely detected in leukemia cells. These results suggest that mutations at codons 61, 71, 72, and 76, in which highest activity at each codon was ten or more, were associated with leukemia (Table 2b; $\chi^2 = 97.0$, $p < 0.001$).

Tartaglia et al. (2003) recently showed that the phosphatase activities of two mutants (D61Y and E76K)

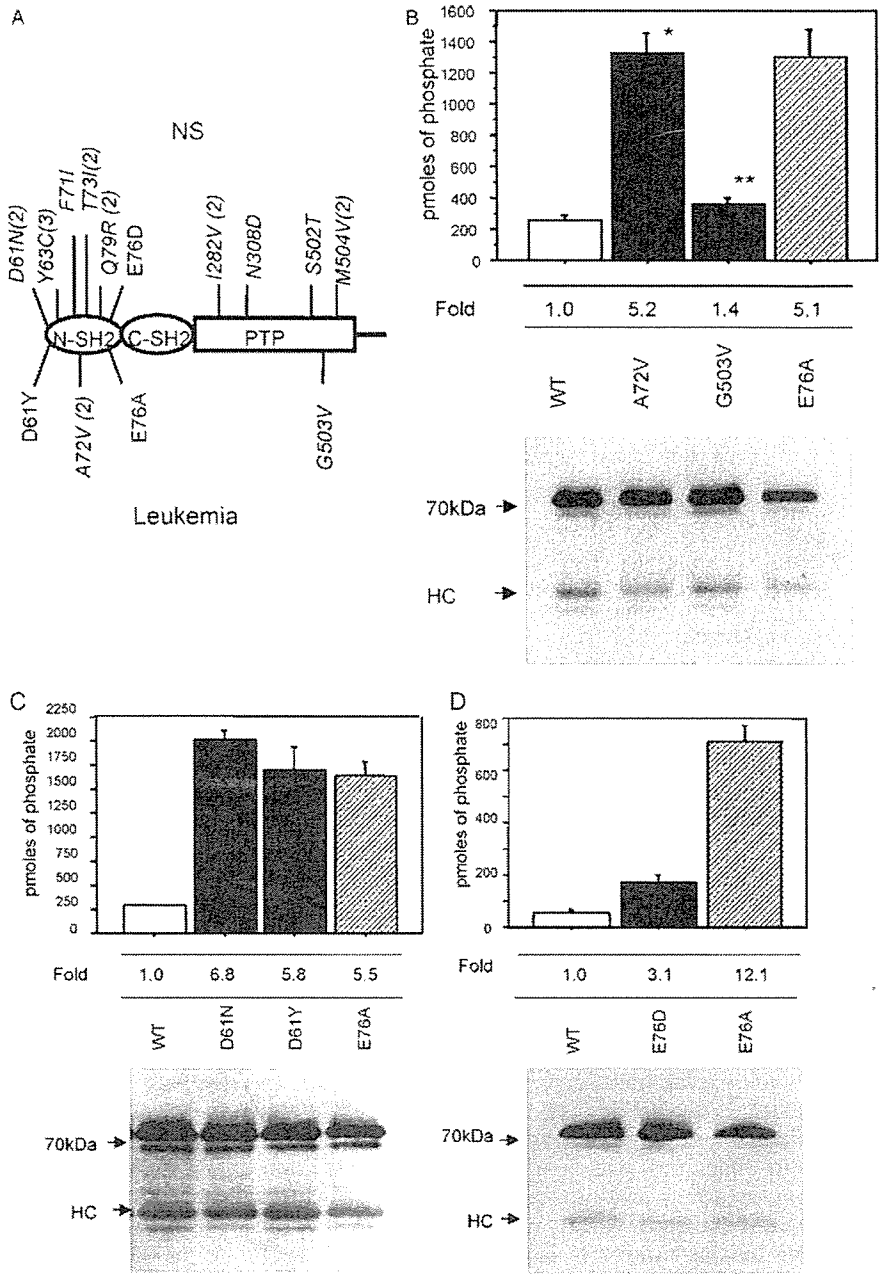

Fig. 2 Phosphatase activity of mutants detected in childhood leukemia. **a** Localization of SHP-2 mutations analyzed in this study. *Italic*, mutations identified in this study. *Parenthesis*, number of patients identified. **b** Immune complex phosphatase assay using SHP-2 mutants identified in leukemia. Results are expressed as mean ± SD obtained from the three independent experiments. *Asterisks* indicate statistically significant differences in activity compared with that of wild type (WT) (* $p < 0.01$, ** $p < 0.05$). **c, d** Comparison of phosphatase activity in mutants derived from either NS or leukemia at amino acid positions 61 and 76. Results are expressed as mean ± SD obtained from the three independent experiments

identified in JMML patients were higher than that of the N308D mutation identified in NS. They put forth a hypothesis explaining the manner in which the two different phenotypes were determined: somatic mutations identified in leukemia have stronger molecular defects and could cause embryonic lethality if they occur in the germline. In contrast, the defects in mutations found in NS patients were milder and insufficient for the development of leukemia. In our experiments, the relative phosphatase activities of D61N (12.1) and F71I (11.8) associated with NS were higher than those of E76A (10) and G503V (2.7) found in leukemia. A comparison of the different substitutions at the same residues showed that the phosphatase activity of D61N (NS) was equivalent to that of D61Y (leukemia). Although Src might not be the physiological substrate of SHP-2 at the developmental stage and leukemogenesis, our results suggest that high phosphatase activity in mutants may not necessarily be associated with embryonic lethality. Further biological studies will be required to explore the mechanisms involved in the development of NS or leukemia.

The F71I mutation in a typical NS patient was inherited from the father, who exhibited only ptosis. The F71I mutation was not detected in 83 controls, and a further functional analysis showed an elevated

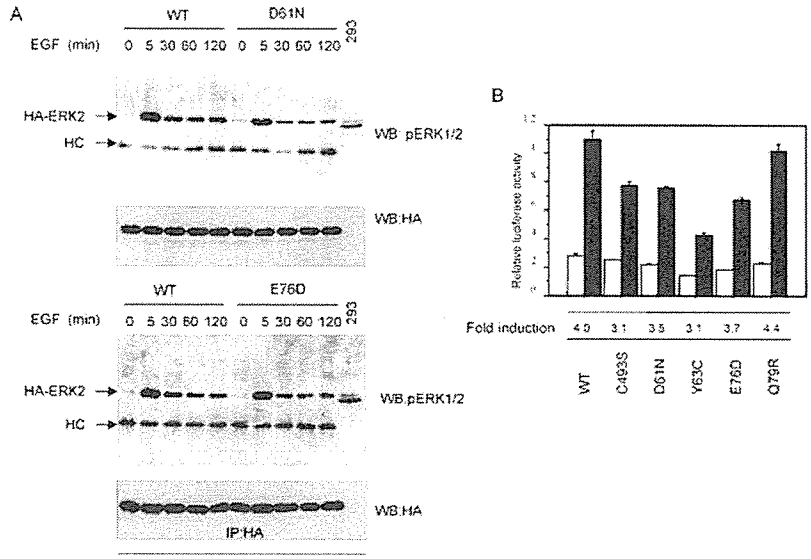

Fig. 3 **a** Effect of the D61N and E76D mutants on extracellular signal-regulated kinase (ERK)2 activation. Lysates were subjected to immunoprecipitation with anti-HA antibody (12CA5), and the immunoprecipitates were subjected to immunoblot analysis with anti-phospho-ERK antibody (*upper panel*). The aliquots of immunoprecipitates were used to confirm that equal amounts of HA-ERK2 were present in each lane (*lower panel*). Cell lysates from epidermal growth factor (EGF)-treated 293 cells were used as a positive control for phospho-ERK(1/2) immunoblotting (293). *HC* heavy chain. *C459S* catalytically inactive mutant. **b** EGF-stimulated transcription of the SRE reporter plasmid in cells expressing wild-type (WT), dominant negative SHP-2, and SHP-2 mutants in the N-SH2 domain. Each value represents luciferase activity in relative light units, which was normalized for Renilla luciferase activity. *White bars*, in the absence of EGF; *filled bars*, in the presence of EGF. Results are expressed as the mean ± SEM of the three independent experiments

phosphatase activity. These observations support the notion that the F71I mutation plays a pathogenic role. One possible explanation for the discrepancy between the clinical and in vitro data is the phenotypic change with age. Allanson et al. (1958) documented the marked change in phenotype with age and reported that manifestations in adults tend to be subtle. Although heart defects and other medical problems had not been observed in the father, it is possible that his facial abnormalities during childhood had been more prominent. Although SHP-2 was essentially expressed in adult organs (Ahmad et al. 1993), in this case, the SHP-2 mutant could have affected specific signaling pathways at the developmental stage. Another possible explanation for his subtle phenotype was due to the poor penetrance of the mutation. Since the genotype–phenotype correlation was not observed in a previous report (Zenker et al. 2004), it is possible that genetic factors other than *PTPN11* are associated with the phenotype of NS.

A recent paper showed that three *PTPN11* mutations were identified in 89 primary neuroblastomas (Bentires-Alj et al. 2004). Two mutations (E69K and T507K) were identified as somatic mutations. Y62C was identified in both tumor and normal adrenal tissues, suggesting that the patient might be NS. In our study, the patient with S502T developed leukocytosis at 3 months of age and neuroblastoma at 6 months of age (Kondoh et al. 2003). Previous reports showed that the insulin-like growth factor or the hepatocyte growth factor stimulated the proliferation or invasion of neuroblastoma cells (Zumkeller and Schwab 1999; Hecht et al. 2004). It is known that SHP-2 regulates these growth-factor signal pathways (Neel et al. 2003). Although the exact mechanisms remain unknown, it is possible that the activated mutations were associated with the pathogenesis of neuroblastoma. It is important to note that the neuroblastoma in the NS patient with the S502T mutation spontaneously disappeared (Kondoh et al. 2003). A similar phenomenon was observed in NS patients associated with JMML, most of which spontaneously resolved (Choong et al. 1999).

A previous report showed that SHP-2 positively regulated the EGF-mediated ERK activation, ELK-1 transactivation, and cell cycle progression in 293 cells (Bennett et al. 1996). In our experiments, two mutations associated with NS failed to promote the RAS/MAPK pathway in the EGF-treated 293 cells. It is controversial as to whether constitutive active mutants lead to enhanced RAS/MAPK pathway. In Xenopus, it was shown that the D61A and E76A mutants induced an elongation of the animal cap. However, this elongation was accompanied by minimal activation of MAPK (O'Reilly et al. 2000). Fragale et al. (2004) reported that mutations such as A72V, I282V, and N308D detected in the NS patients caused prolonged binding of GAB1, a binding partner of SHP-2, and sustained ERK activation when GAB1 was cointroduced in EGF-treated COS cells. In contrast, ERK was not hyperactivated in Ba/F3 cells expressing mutants associated with JMML (D61G and E76K) although these cells showed enhanced growth-factor-independent survival. A recent study analyzing knock-in mice expressing the D61G mutation showed cell- and pathway-specific EKR activation in the developing mice

Table 2a Comparison of the phosphatase activities of mutants and the phenotype in patients. Relative phosphatase activities and number of patients at each residue were shown. Patients with NS and leukemia reported previously were summarized on selected residues where phosphatase activity was measured in this study. References are as follows; 1, (Tartaglia et al. 2002); 2, (Musante et al. 2003); 3, (Loh et al. 2004); 4, (Kosaki et al. 2002); 5, (Zenker et al. 2004); 6, (Yoshida et al. 2004); 7, (Tartaglia et al. 2003); 8, (Tartaglia et al. 2004); 9, (Maheshwari et al. 2002); 10, (Sarkozy et al. 2003); 11, (Schollen et al. 2003). *WT* wild type, *NS* Noonan syndrome, *JMML* juvenile myelomonocytic leukemia, *MDS* myelodysplastic syndrome, *AML* acute myeloid leukemia, *ALL* acute lymphoid leukemia

Domain	Exon	Codon	WT	Mutation	Relative phosphatase activity[a]	NS	NS/JMML NS (germline)	JMML non-NS (somatic)	MDS	AML	ALL	References
N-SH2	3	61	Asp	Asn	**12.1**	4		1				1–3, our study
				Gly		8						1, 2, 4–6
				Tyr	**10.5**			6		1	1	3, 7, 8
				Val					2		1	3, 7, 8
N-SH2	3	63	Tyr	Cys	**2.5**	23		1				1–6, 9, 10, our study
N-SH2	3	71	Phe	Leu		1			1			2, 7
				Ile	**11.8**	1						our study
				Lys					2			3, 7
N-SH2	3	72	Ala	Ser		4						2, 4, 5
				Gly		4						1, 5, 10
				Thr				3			1	3, 7, 8
				Val	**10.2**			3	2	3	3	3, 7, 8, our study
				Asp							1	8
N-SH2	3	73	Thr	Ile	**6.0**	9	7					1–7, our study
N-SH2	3	76	Glu	Asp	**2.4**	3		1				1–3, 5
				Lys				4		2	4	3, 7, 8
				Val				1				7
				Gly				2		1	2	3, 7, 8
				Ala	**10**			1	1			7
				Gln				1			2	3, 8
N-SH2	3	79	Gln	Arg	**2.1**	14						1, 2, 5, 6, 11, our study
				Pro		1						10
PTP	7	282	Ile	Val	**6.3**	4						1, 2, our study
PTP	8	308	Asn	Asp	**3.2**	37						1, 2, 5, 6, 10, our study
				Ser		7						1, 4, 5, 10
PTP	13	502	Ser	Thr	**5.6**	4						6, 9, our study
				Pro						1		8
PTP	13	503	Gly	Arg		3	1					5, 7, 10
				Ala				1				7
				Val	**2.7**			1				our study
PTP	13	504	Met	Val	**6.1**	7						1, 5, 10, our study

[a] Variation of each assay was normalised; activity of WT cDNA was taken as 1 and that of E76A was taken as 10

Table 2b Highest r-phosphatase activity at each codon and patients' phenotype

Highest r-phosphatase activity in mutations at the codon	Codon	NS, NS/JMML (germline mutation)	JMML, MDS, AML, ALL (somatic mutation)
> 10, 10	61, 71, 72, 76	25	53
< 10	63, 73, 79, 282, 308, 502, 503, 504	117	4

(Araki et al. 2004). These experiments and our data suggest that the manner in which the constitutive active mutants regulate their downstream signaling pathway(s) depends on cell types and signaling pathways.

In conclusion, we showed that the phosphatase activity of 14 mutations identified in NS and leukemia was elevated to various degrees. High phosphatase activity in mutations at codons 61, 71, 72, and 76 was associated with leukemogenesis. A further analysis of the downstream signals of the mutants would provide the key to elucidate the role of *PTPN11* mutations in patients with NS and leukemia.

Acknowledgements The authors thank the patients and their families who participated in this study and doctors who referred the cases. We are grateful to Dr. Takashi Matozaki, Gunma University, for supplying pcDNA-HAERK2 plasmid and anti-HA antibody, and Dr. Jun-ichi Miyazaki, Osaka University, for supplying the pCAGGS expression vector. We thank Kumi Kato, Dr. Xue Yang, and Dr. Yoshio Takahashi for their technical assistance. This work was supported by Grants-in-Aid from the Ministry of Education, Culture, Sports, Science and Technology of Japan (No.15790172) and the Uehara Memorial Foundation Grant-in-Aid for Scientific Research to YA.

References

Ahmad S, Banville D, Zhao Z, Fischer EH, Shen SH (1993) A widely expressed human protein-tyrosine phosphatase containing src homology 2 domains. Proc Natl Acad Sci USA 90:2197–2201

Allanson JE (1987) Noonan syndrome. J Med Genet 24:9–13

Allanson JE, Hall JG, Hughes HE, Preus M, Witt RD (1985) Noonan syndrome: the changing phenotype. Am J Med Genet 21:507–514

Aoki Y, Huang Z, Thomas SS, Bhide PG, Huang I, Moskowitz MA, Reeves SA (2000) Increased susceptibility to ischemia-induced brain damage in transgenic mice overexpressing a dominant negative form of SHP2. Faseb J 14:1965–1973

Araki T, Mohi MG, Ismat FA, Bronson RT, Williams IR, Kutok JL, Yang W, Pao LI, Gilliland DG, Epstein JA, Neel BG (2004) Mouse model of Noonan syndrome reveals cell type- and gene dosage-dependent effects of Ptpn11 mutation. Nat Med 10:849–857

Bennett AM, Hausdorff SF, O'Reilly AM, Freeman RM, Neel BG (1996) Multiple requirements for SHPTP2 in epidermal growth factor-mediated cell cycle progression. Mol Cell Biol 16:1189–1202

Bentires-Alj M, Paez JG, David FS, Keilhack H, Halmos B, Naoki K, Maris JM, Richardson A, Bardelli A, Sugarbaker DJ, Richards WG, Du J, Girard L, Minna JD, Loh ML, Fisher DE, Velculescu VE, Vogelstein B, Meyerson M, Sellers WR, Neel BG (2004) Activating mutations of the noonan syndrome-associated SHP2/PTPN11 gene in human solid tumors and adult acute myelogenous leukemia. Cancer Res 64:8816–8820

Choong K, Freedman MH, Chitayat D, Kelly EN, Taylor G, Zipursky A (1999) Juvenile myelomonocytic leukemia and Noonan syndrome. J Pediatr Hematol Oncol 21:523–527

Feng GS (1999) Shp-2 tyrosine phosphatase: signaling one cell or many. Exp Cell Res 253:47–54

Fragale A, Tartaglia M, Wu J, Gelb BD (2004) Noonan syndrome-associated SHP2/PTPN11 mutants cause EGF-dependent prolonged GAB1 binding and sustained ERK2/MAPK1 activation. Hum Mutat 23:267–277

Hakak Y, Martin GS (1999) Cas mediates transcriptional activation of the serum response element by Src. Mol Cell Biol 19:6953–6962

Hecht M, Papoutsi M, Tran HD, Wilting J, Schweigerer L (2004) Hepatocyte growth factor/c-Met signaling promotes the progression of experimental human neuroblastomas. Cancer Res 64:6109–6118

Hof P, Pluskey S, Dhe-Paganon S, Eck MJ, Shoelson SE (1998) Crystal structure of the tyrosine phosphatase SHP-2. Cell 92:441–450

Kondoh T, Ishii E, Aoki Y, Shimizu T, Zaitsu M, Matsubara Y, Moriuchi H (2003) Noonan syndrome with leukaemoid reaction and overproduction of catecholamines: a case report. Eur J Pediatr 162:548–549

Kosaki K, Suzuki T, Muroya K, Hasegawa T, Sato S, Matsuo N, Kosaki R, Nagai T, Hasegawa Y, Ogata T (2002) PTPN11 (protein-tyrosine phosphatase, nonreceptor-type 11) mutations in seven Japanese patients with Noonan syndrome. J Clin Endocrinol Metab 87:3529–3533

Loh ML, Vattikuti S, Schubbert S, Reynolds MG, Carlson E, Lieuw KH, Cheng JW, Lee CM, Stokoe D, Bonifas JM, Curtiss NP, Gotlib J, Meshinchi S, Le Beau MM, Emanuel PD, Shannon KM (2004) Mutations in PTPN11 implicate the SHP-2 phosphatase in leukemogenesis. Blood 103:2325–2331

Maheshwari M, Belmont J, Fernbach S, Ho T, Molinari L, Yakub I, Yu F, Combes A, Towbin J, Craigen WJ, Gibbs R (2002) PTPN11 mutations in Noonan syndrome type I: detection of recurrent mutations in exons 3 and 13. Hum Mutat 20:298–304

Mendez HM, Opitz JM (1985) Noonan syndrome: a review. Am J Med Genet 21:493–506

Musante L, Kehl HG, Majewski F, Meinecke P, Schweiger S, Gillessen-Kaesbach G, Wieczorek D, Hinkel GK, Tinschert S, Hoeltzenbein M, Ropers HH, Kalscheuer VM (2003) Spectrum of mutations in PTPN11 and genotype-phenotype correlation in 96 patients with Noonan syndrome and five patients with cardio-facio-cutaneous syndrome. Eur J Hum Genet 11:201–206

Neel BG, Gu H, Pao L (2003) The 'Shp'ing news: SH2 domain-containing tyrosine phosphatases in cell signaling. Trends Biochem Sci 28:284–293

Niwa H, Yamamura K, Miyazaki J (1991) Efficient selection for high-expression transfectants with a novel eukaryotic vector. Gene 108:193–199

O'Reilly AM, Pluskey S, Shoelson SE, Neel BG (2000) Activated mutants of SHP-2 preferentially induce elongation of Xenopus animal caps. Mol Cell Biol 20:299–311

Sarkozy A, Conti E, Seripa D, Digilio MC, Grifone N, Tandoi C, Fazio VM, Di Ciommo V, Marino B, Pizzuti A, Dallapiccola B (2003) Correlation between PTPN11 gene mutations and congenital heart defects in Noonan and LEOPARD syndromes. J Med Genet 40:704–708

Schollen E, Matthijs G, Gewillig M, Fryns JP, Legius E (2003) PTPN11 mutation in a large family with Noonan syndrome and dizygous twinning. Eur J Hum Genet 11:85–88

Servidei T, Aoki Y, Lewis SE, Symes A, Fink JS, Reeves SA (1998) Coordinate regulation of STAT signaling and c-fos expression by the tyrosine phosphatase SHP-2. J Biol Chem 273:6233–6241

Takeda H, Matozaki T, Takada T, Noguchi T, Yamao T, Tsuda M, Ochi F, Fukunaga K, Inagaki K, Kasuga M (1999) PI 3-kinase gamma and protein kinase C-zeta mediate RAS-independent activation of MAP kinase by a Gi protein-coupled receptor. EMBO J 18:386–395

Tartaglia M, Mehler EL, Goldberg R, Zampino G, Brunner HG, Kremer H, van der Burgt I, Crosby AH, Ion A, Jeffery S, Kalidas K, Patton MA, Kucherlapati RS, Gelb BD (2001) Mutations in PTPN11, encoding the protein tyrosine phosphatase SHP-2, cause Noonan syndrome. Nat Genet 29:465–468

Tartaglia M, Kalidas K, Shaw A, Song X, Musat DL, van der Burgt I, Brunner HG, Bertola DR, Crosby A, Ion A, Kucherlapati RS, Jeffery S, Patton MA, Gelb BD (2002) PTPN11 mutations in Noonan syndrome: molecular spectrum, genotype-phenotype correlation, and phenotypic heterogeneity. Am J Hum Genet 70:1555–1563

Tartaglia M, Niemeyer CM, Fragale A, Song X, Buechner J, Jung A, Hahlen K, Hasle H, Licht JD, Gelb BD (2003) Somatic mutations in PTPN11 in juvenile myelomonocytic leukemia, myelodysplastic syndromes and acute myeloid leukemia. Nat Genet 34:148–150

Tartaglia M, Martinelli S, Cazzaniga G, Cordeddu V, Iavarone I, Spinelli M, Palmi C, Carta C, Pession A, Arico M, Masera G, Basso G, Sorcini M, Gelb BD, Biondi A (2004) Genetic evidence for lineage-related and differentiation stage-related contribution of somatic PTPN11 mutations to leukemogenesis in childhood acute leukemia. Blood 104:307–313

Yoshida R, Hasegawa T, Hasegawa Y, Nagai T, Kinoshita E, Tanaka Y, Kanegane H, Ohyama K, Onishi T, Hanew K, Okuyama T, Horikawa R, Tanaka T, Ogata T (2004) Protein-tyrosine phosphatase, nonreceptor type 11 mutation analysis and clinical assessment in 45 patients with noonan syndrome. J Clin Endocrinol Metab 89:3359–3364

Zenker M, Buheitel G, Rauch R, Koenig R, Bosse K, Kress W, Tietze HU, Doerr HG, Hofbeck M, Singer H, Reis A, Rauch A (2004) Genotype-phenotype correlations in Noonan syndrome. J Pediatr 144:368–374

Zumkeller W, Schwab M (1999) Insulin-like growth factor system in neuroblastoma tumorigenesis and apoptosis: potential diagnostic and therapeutic perspectives. Horm Metab Res 31:138–141

Electrophysiological and Histopathological Characteristics of Progressive Atrioventricular Block Accompanied by Familial Dilated Cardiomyopathy Caused by a Novel Mutation of Lamin A/C Gene

JUN OTOMO, M.D., SHIGEO KURE, M.D.,* TOMOKO SHIBA, M.D., AKIHIKO KARIBE, M.D., TSUYOSHI SHINOZAKI, M.D., TETSUO YAGI, M.D.,† HIROSHI NAGANUMA, M.D.,‡ FUMIAKI TEZUKA, M.D.,§ MASAETSU MIURA, M.D.,¶ MEIICHI ITO, M.D.,‖ JUN WATANABE, M.D., YOICHI MATSUBARA, M.D.,* and KUNIO SHIRATO, M.D.

From the Departments of Cardiovascular Medicine and *Medical Genetics, Tohoku University Graduate School of Medicine, Sendai; †Department of Cardiovascular Medicine and ‡Pathology, Sendai City Hospital, Sendai; §Department of Pathology, National Sendai Hospital, Sendai; ¶Department of Cardiovascular Medicine, Furukawa City Hospital, Furukawa; and ‖Ito Clinic, Kami, Japan

Conduction Defect Caused by Lamin A/C Gene Mutation. ***Introduction:*** **Mutations of lamin A/C gene (*LMNA*) cause dilated cardiomyopathy (DCM) with atrioventricular (AV) conduction defect, although the electrophysiological and histological profiles are not fully understood.**

Methods and Results: **We analyzed a large Japanese family (21 affected and 203 unaffected members) of DCM with AV block. The responsible *LMNA* mutation of IVS3–10A>G was novel and caused an aberrant splicing. The first clinical manifestation was low-grade AV block or atrial fibrillation (AF), which developed in affected members aged ≥30 years. We observed that the AV block progressed to third-degree within several years. The electrophysiological study of the four affected members revealed an impairment of intra-AV nodal conduction. Because of advanced AV block, pacemakers were implanted in 14 out of 21 affected members at the mean age of 44 years. Three affected members died suddenly and two affected members died of heart failure and/or ventricular tachycardia (VT) even after the pacemaker implantation. Postmortem examination showed conspicuous fibrofatty degeneration of the AV node. Endomyocardial biopsies showed remarkably deformed nuclei and substantial glycogen deposits in the subsarcolemma.**

Conclusion: **The clinical phenotype in this family was characterized by (1) the first manifestation of the prolonged PQ interval or AF in adolescence, (2) progressive intra-AV nodal block to the third degree in several years, and (3) progressive heart failure after pacemaker implantation. Histological study revealed preferential degeneration at the AV node area and novel cellular damages in the working myocardium.**
(J Cardiovasc Electrophysiol, Vol. 16, pp. 137-145, February 2005)

lamin A/C, dilated cardiomyopathy, atrioventricular block, atrial fibrillation, gene

Introduction

Two polypeptides, lamin A and lamin C, are encoded by the lamin A/C gene (*LMNA*). These arise through alternative splicing of the same primary transcript.[1,2] Lamin A and lamin C proteins are components of the nuclear envelope, forming the inner and the outer nuclear membranes, the nuclear pore complex, and the nuclear lamina.[3] It has been reported that mutations in the *LMNA* cause various genetic diseases referred to as "laminopathy."[4] To date, seven different types of laminopathies have been established: autosomal dominant[5]/recessive[6] Emery-Dreifuss muscular dystrophy, limb-girdle muscular dystrophy 1B,[7] familial partial lipodystrophy,[8] sensory and motor axonal neuropathy Charcot-Marie-Tooth disorder type 2,[9] mandibuloacral dysplasia,[10] Hutchinson-Gilford progeria syndrome,[11] and autosomal dominant dilated cardiomyopathy (DCM) with conduction defect.[12]

The laminopathies have two major cardiac phenotypes, progressive atrioventricular (AV) block, and myocardial damage. The AV block in the laminopathies is mostly accompanied by cardiomyopathy, but isolated AV block was reported in limb girdle muscular dystrophy 1B[7,13] and autosomal dominant DCM with conduction defect.[14] We found a large family with DCM with progressive AV block caused by a novel mutation of *LMNA* and provide the clinical, genetic, electrophysiological, and histopathological findings concerning this particular familial DCM.

Methods

Participation of the Family

This familial DCM was first identified by the high incidence of pacemaker implantation (PMI). We started the investigation of the family because the preliminary study revealed a

This study was supported by a grant from the Ministry of Education, Culture, Sports, Science, and Technology, and a grant from the Ministry of Health, Labor, and Public Welfare.

Address for correspondence: Jun Watanabe, M.D., Department of Cardiovascular Medicine, Tohoku University Graduate School of Medicine, 1-1, Seiryo-machi, Aoba-ku, Sendai, 980-8574, Japan. Fax: +81-22-717-7156; E-mail: watanabe@cardio.med.tohoku.ac.jp

Manuscript received 1 March 2004; Revised manuscript received 11 September 2004; Accepted for publication 20 September 2004.

doi: 10.1046/j.1540-8167.2004.40096.x

high incidence of not only PMI but also DCM (Fig. 1A). Written informed consent was obtained from all participants under approval of the local ethics committee. The family members showing DCM on echocardiogram were designated as affected irrespective of the presence of the conduction defect. The members who died suddenly or died of heart failure without otherwise known causes were also regarded as affected. We collected clinical data of the affected members from the medical records, which included 12-lead electrocardiogram (ECG), transthoratic echocardiogram, and serum creatine kinase. The data of cardiac catheterization and postmortem examination were also evaluated when available. Neurological assessment was performed for clinically affected members by review of medical records, blood examination of serum creatine kinase, and clinical neuromuscular examination evaluated by neurological experts. The family members (≥30 years of age) showing no cardiac phenotypes were designated as unaffected. We examined ECG, echocardiogram, and serum creatine kinase in some unaffected members.

Mutational Analysis of LMNA

We obtained 5–10 mL blood samples from each family member. Genomic DNA was extracted from the whole blood in 25 family members or heart tissue obtained at autopsy. Because the *LMNA*-mutated DCM with conduction defect was known, we first screened for mutations of *LMNA*.[12] Twelve coding exons of *LMNA* were amplified by polymerase chain reaction (PCR) in the proband (IV-70 in Fig. 1A) as described.[12] Direct sequencing analysis was performed with an automated fluorescence sequencer (ABI PRISM 310, PE-Biosystems, Foster City, CA) by the dye-primer cycle sequencing method as described.[15] The PCR-based restriction fragment length polymorphism (PCR-RFLP) analysis was performed in family members and in 100 chromosomes from 50 normal volunteers (randomly selected from our control genomic store, ≥30 years of age) to test whether the mutation was a polymorphism by using a modified forward primer, 5′-CCAGCACTCAGCTCCCAGGT-3′ and a reverse primer, 3′-TGGTCTCACGCAGCTCCTGGAAGCG-5′. The underlined nucleotide represents an introduced mismatch, which generated a recognition site for *HhaI* in DNA fragments amplified from the mutant allele. The thermoprofile consisted of initial denaturing of 95°C for 3 min, 35 cycles of 98°C or 10 seconds, 55°C for 30 seconds, and 72°C for 30 seconds, followed by 72°C for 7 min. A total of 10 μL of PCR products were digested with 10 units of *HhaI* at 37°C overnight followed by 4% agarose gel electrophoresis. The DNA flagments were stained with ethidium bromide and visualized on a UV transilluminator.

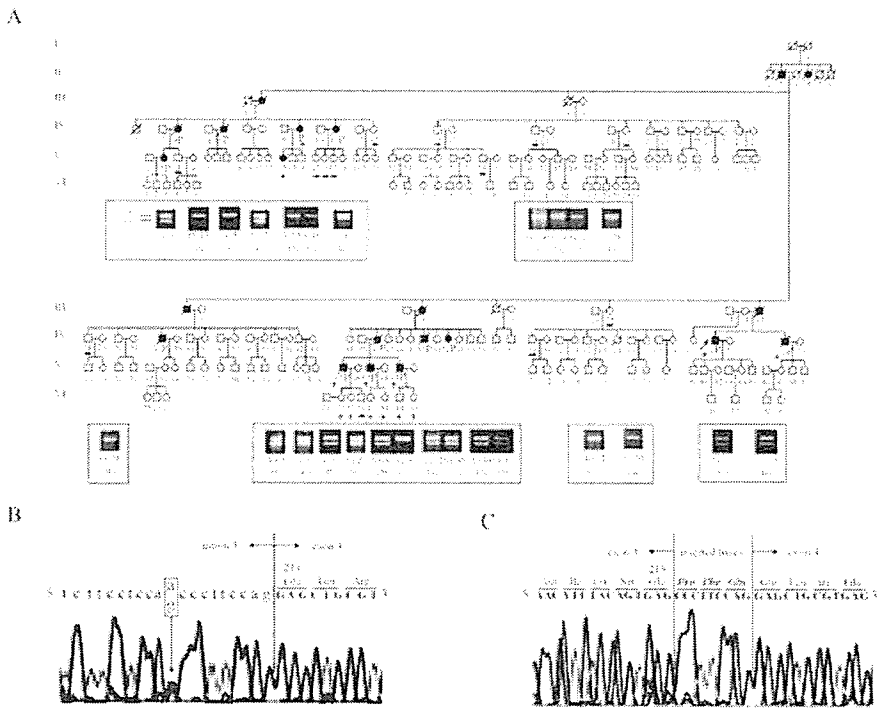

Figure 1. *The family pedigree and LMNA mutation. (A) The family pedigree with DCM with conduction defect caused by the LMNA mutation. Circles and squares indicate male and female, respectively. Closed circles and squares indicate affected members. Roman and arabic numerals indicate generation and case numbers. The letter P indicates affected members who received pacemaker implantation. Slash means deceased. Plus and minus indicate presence and absence of the mutation, IVS3–10A>G, respectively. An arrow indicates the proband. The photographs in boxes show electrophoresis of HhaI-digested PCR by PCR-RFLP analysis. Two DNA fragments of 156 bp and 134 bp show the presence of the mutation, IVS3–10A>G, while only the fragment of 156 bp shows the absence of the mutation. (B) Direct sequencing analysis of the LMNA mutation. The proband had a heterozygous base substitution from adenine (a) to guanine (g) at 10-base upstream from the junction between intron 3 and exon 4 (IVS3–10A>G, arrow points). Numbers above the amino acid symbols indicate the codon number. (C) A cDNA analysis of the LMNA mutation. Direct sequencing analysis of a cDNA fragment of 158 bp reveals insertion of nine bases, 5′-CCCTTCCAG-3′, in the junction between exon 3 and exon 4. Amino acid symbols in bold and italic represent three codons inserted into the exon 3/exon 4 junction.*

Analysis of LMNA mRNA of a Lymphoblast Cell Line Established from a Patient

A lymphoblast cell line was established from a blood sample of the proband by Epstein-Barr virus infection. Total RNA was purified from the lymphoblasts with RNeasy Mini kit (Qiagen, Germany) and subjected to reverse transcription as described.[15] A cDNA fragment containing the exon 3/exon 4 junction was amplified by PCR with a forward primer, 5′-GAGAACAGGCTGCAGACCAT-3′, and a reverse primer, 3′-TTGTCAATCTCCACCAGTC G-5′. The RT-PCR products were size-separated by 5% NuSieve GTG agarose (FMC BioProducts, Rockland) gel electrophoresis, and cDNA fragments of 149 bp and 158 bp in size were excised for direct sequencing analysis as described above.

Electrophysiological and Histological Examination

Conventional electrophysiological (EP) study was performed in four affected members because of AV block. Three standard electrode catheters were positioned in the high right atrium, His bundle region, and RV. A quadripolar-catheter or octapolar-catheter was inserted into the coronary sinus and positioned to record the coronary sinus electrogram using each pair of electrodes. The EP study included standard diagnostic protocols for sinus nodal function, AV nodal function, and ventricular tachycardia (VT) induction.[16] Briefly, in the induction of VT, up to three extrastimuli were induced (coupling intervals $\geq$ 180 ms) from the apex and the outflow tract of the RV after conditioning pacing (basic cycle length = 600 or 400 ms). If negative, we repeated the protocol above under intravenous administration of isoproterenol (started at 0.5 μg/min, a target heart rate was 20% increase from the control).[17]

Histopathological examination was performed in two postmortem heart samples obtained from affected members (IV-72, V-65) and in four biopsied samples of endomyocardial tissues taken from the septum and apex of the RV. Light and electron microscopical analysis was performed.

Results

Clinical Characteristics of Affected Family Members

The clinical characteristics of 21 affected members are summarized in Table 1. Information concerning the first manifestation was available in six affected members: first- or second-degree AV block and/or atrial fibrillation (AF) initially developed in five of the six affected members, IV-70, V-12, V-65, V-67, and V-69, while affected member IV-72 presented congestive heart failure with AF and third-degree

TABLE 1

Clinical Characteristics of Clinically Affected Members in the Family with Lamin A/C Gene Mutation

		Clinical Course			Echocardiogram					
Case No.	Gender	Onset (age)	PMI (age)	Cause of Death (age)	Age	LVEDD/ ESD (mm)	LVEF (%)	LAD (mm)	MD	Comment
II-2*	M	ND	No	53 y CHF					ND	
II-4*	F	ND	No	51 y SD					ND	
III-2*	F	ND	No	58 y CHF					ND	
III-5*	M	ND	No	55 y CHF					ND	
III-8*	F	ND	No	45 y SD					ND	
III-15*	M	ND	No	59 y CHF					ND	
IV-3*	F	ND	50 y	71 y cause unknown					ND	
IV-5*	F	ND	50 y	59 y apoplexy					ND	
IV-9	F	ND	49 y	64 y live					ND	
IV-11*	F	ND	40 y	58 y CHF and VT					ND	
IV-32*	M	ND	37 y	55 y SD					ND	
IV-46*	F	ND	45 y	62 y SD					ND	
IV-50*	M	ND	Yes	Age and cause unknown					ND	
IV-52*	F	ND	Yes	Live; age unknown					ND	
IV-70	M	42 y first- to second-degree AVB and AF (QRS = 0.10 sec)	45 y high-degree AVB and AF	53 y live	42 y 45 y 53 y	55/38 61/42 61/45	68 69 60	35 38 47	NM	43 y Holter ECG; four consecutive PVCs CK 79 (mU/mL) (<197 mU/mL)
IV-72	M	47 y CHF and third-degree AVB with AF (QRS = 0.10 sec)	47 y third-degree AVB with AF	50 y SD	47 y 49 50	69/56 66/65 76/67	36 33 24	55 55 58	NM	Diabetes mellitus, 48 y spontaneous sustained VT, CK 155 (mU/mL) (<200 mU/mL)
V-2*	F	ND	38 y	54 y live					ND	DCM
V-12	F	41 y first-degree AVB (PR = 0.22 sec, QRS = 0.08 sec)	No	42 y live	41 y	43/30	65	23	NM	41 y Holter ECG; couplet PVCs, Ergometer; PVC increased
V-65	M	42 y paroxysmal AF (QRS = 0.10 sec)	45 y high-degree AVB and AF	48 y CHF and VT	45 y 48 y	59/44 60/53	51 23	42 43	NM	47 y spontaneous sustained VT (LBBB+inferior axis type) CK 134 (mU/mL) (<195 mU/mL)
V-67	M	37 y paroxysmal AF (QRS = 0.10 sec)	43 y high-degree AVB and AF	49 y live	43 y 47 y	56/47 62/43	31 58	43 49	NM	47 y spontaneous sustained VT (RBBB+superior axis type) CK 134 (mU/mL) (<195 mU/mL)
V-69	M	30 y first- to second-degree AVB (QRS = 0.11 sec)	37 y third-degree AVB	47 y live	39 y 44 y	52/45 60/47	31 41	43 41	NM	38 y spontaneous sustained VT (RBBB+inferior axis type) 42 y performed catheter ablation for VT, CK 49 (mU/mL) (< 195 mU/mL)

*Clinically affected member whose DNA was not available for the study.

AF = atrial fibrillation; AVB = atrioventricular block; CHF = congestive heart failure; CK = creatine kinase; DCM = dilated cardiomyopathy; F = female; LAD = left atrial diameter; LBBB = left bundle branch block; LVEDD/ESD = left ventricular end-diastolic/end-systolic diameter; LVEF = left ventricular ejection fraction; M = male; MD = skeletal muscle disorder; ND = not detectable; y = year; NM = no manifestation; PMI = permanent pacemaker implantation; PVC = premature ventricular contraction; RBBB = right bundle branch block; SD = sudden death; VT = ventricular tachycardia.

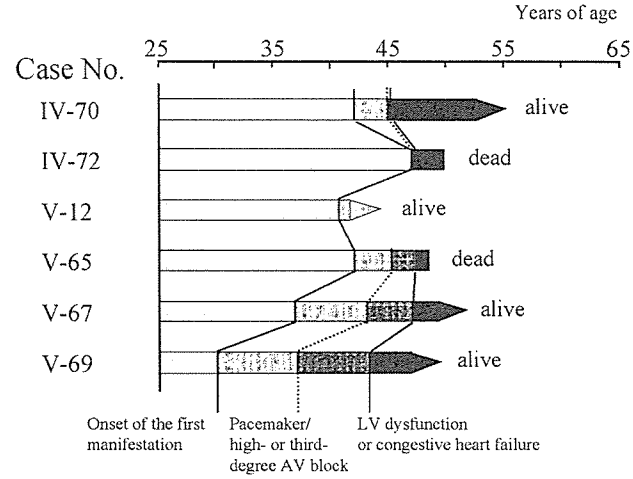

Figure 2. *Onset and time course of AV block and LV dysfunction. The onset and the time course of AV block and LV dysfunction are illustrated. The first manifestation, including first- or second-degree AV block and/or AF, occurred at 30 to 47 years of age. In four out of six affected members, AV block progressed to third-degree AV block, and these members received pacemaker implantation within 3 to 7 years. In two dead affected members, the first manifestation was more likely to occurr later and progressed rapidly. LV dysfunction was defined by LV diameter ≥ 60 mm or LV ejection fraction ≤ 40%.*

AV block at the onset of the disease (Fig. 2). The age of onset ranged from 30 to 47 years with a mean age of 40 years. At the first manifestations, all affected members had normal width of QRS complex, and intraventricular conduction delay was not found. Because of the progression to advanced AV block, 14 of the 21 the affected members received pacemakers, and six affected members died before pacemakers were clinically available. One affected member, V-12, was 42 years old and had only first-degree AV block. The mean age of PMI was 44 years with a range of 37–50 years. The PMI was needed within 7 years from the first manifestations such as first- or second-degree AV block and/or AF (Fig. 2). The width of QRS complex remained normal at the PMI. Fourteen of the 21 affected members have died, and the affected members with pacemakers died at a mean age of 57 (48–71) years, while the affected members without pacemakers died at a mean age of 53 (45–59) years. Sudden death was observed in five of these 14 affected members and six affected members died of congestive heart failure or fatal VT. The affected members, IV-70, V-12, V-65, V-67, and V-69, showed no clinical symptoms of congestive heart failure at the first manifestation. In affected members, IV-70 and V-12, echocardiography revealed normal LV dimensions and cardiac function. After the first manifestation, affected member IV-70 showed the progression of LV dilatation within 3 years. Echocardiogarphical LV dysfunction (LV diameter ≥ 60 mm, or LV ejection fraction ≤40%) was found 6 years after the first manifestation in affected member V-65, 6 years later in affected member V-67, and 9 years later in affected member V-69. The affected member, IV-72, first visited a hospital for clinical heart failure with third-degree AV block. No documentation was available concerning whether heart failure was followed by AV block (Fig. 2). In the general neurological assessment, no skeletal muscle abnormalities were found by neurological experts or in the review of medical records of clinically affected members in the family. Four genetically affected members (IV-70, IV-72, V-65, and V-69) were extensively evaluated by neurological experts and no manifestation such as Emery-Dreifuss muscular dystropy, limb-girdle muscular dystrophy, or Charcot-Marie-Tooth disorder was found. Serum creatine kinase was within the normal range in some affected members (IV-70, IV-72, V-65, and V-69).

Identification of LMNA Mutation

All coding regions of *LMNA* were screened for mutations in a DNA sample of the proband (IV-70). Direct sequencing analysis did not reveal any base change in each exon, but a heterozygous base substitution from adenine to guanine was detected 10-base upstream of the intron 3/exon 4 junction (IVS3–10A>G) (Fig. 1B). We screened for the IVS3–10A>G by direct sequencing and PCR-RFLP analysis in 19 members (≥30 years of age), which included seven affected (IV-9, IV-70, IV-72, V-12, V-65, V-67, V-69) and 12 unaffected members (III-12, IV-13, IV-14, IV-16, IV-19, IV-28, IV-58, V-3, V-15, V-16, V-17, V-28), and in seven members (<30 years of age) showing no cardiac phenotype (VI-29, VI-30, VI-31, VI-32, VI-33, VI-34, VI-35) whose fathers are affected members. The IVS3–10A>G mutation was detected in all the seven members, but not in all the 12 unaffected members. Furthermore, the mutation was detected in six of the seven members (<30 years of age) showing no cardiac phenotype. Results of the PCR-RFLP analysis are shown in Figure 1A. On the other hand, the mutation was not detected in 100 control alleles (data not shown). These results suggested that the mutation was tightly associated with the disease and that there were mutant carriers (<30 years of age) before the onset of the disease.

The RT-PCR study revealed two cDNA fragments of 149 and 158 bp in size in the proband (data was not shown), while only the 149-bp fragment was observed in the control (data was not shown). Direct sequencing analysis showed that a nine-base fragment, 5′-CCCTTCCAG-3′, was inserted in the junction between exon 3 and exon 4 in the 158-bp fragments (Fig. 1C). These results suggested that the IVS3–10A > G altered a splicing site to the 10th nucleotide (a/g heterozyzous) upstream from the 3′ end of the intron 3 from the junction between the intron 3 and exon 4 (Fig. 1B).

TABLE 2

Electrophysiological Characteristics of Affected Members with Lamin A/C Gene Mutation

Case No.	Gender	Age	Electrophysiological Conductive Parameters							Induced Arrythmia	
			P Duration (ms)	PR Interval (ms)	PA Interval (ms)	AH Interval (ms)	HV Interval (ms)	QRSS Duration (ms)	Wenckebach Rate at Atrial Pacing (beats/min)	Atrial Arrhythmia	Ventricular Arrhythmia
IV-70	M	45	110	470	30	370	55	100	100	AF (before EPS)	NP
V-65	M	45	120	565	30	460	55	100	50	AF (before EPS)	Sustained VT (LBBB+inferior axis type)
V-67*	M	43	AF	AF	AF	AF	50	100	AF	AF	NI
V-69	M	42	140	Wenckebach	80	Wenckebach	40	110	During sinus rhythm	NP	Sustained VT (RBBB+inferior axis type)

* During sinus rhythm before EPS, administration of 1.0 mg of atropine sulphate improved Wenckebach-type AV block to one to one AV conduction.
AF = atrial fibrillation; EPS = electrophysiological study; LBBB = left bundle branch block; M = male; NI = not induced; NP = not performed; RBBB = right bundle branch block; VT = ventricular tachyardia.

Electrophysiological and Histopathological Characteristics

EP study was performed in four affected members, IV-70, V-65, V-67, and V-69, because of bradycardia and/or spontaneous VT (Table 2). The EP study indicated that affected members, IV-70 and V-65, had AV nodal dysfunction with marked prolongation of the AH interval. In contrast, the HV interval and QRS duration were normal in all four affected members, indicating that the conduction systems of the infra-His bundle to Purkinje fiber and intraventricles might not be impaired. Although affected member, V-65, had AF (Fig. 3A), the AV conductivity was evaluated after DC defibrillation. He demonstrated Wenckebach-type second-degree AV block (Fig. 3B) with prolonged AH interval (Fig. 3C). Furthermore, VT could be reproducibly induced by programmed stimulation to the outflow tract of the RV (Fig. 3D).

Heart specimens were obtained at autopsy from affected members, IV-65 and V-72. Microscopical examination disclosed marked fibrofatty degeneration in the AV junction and

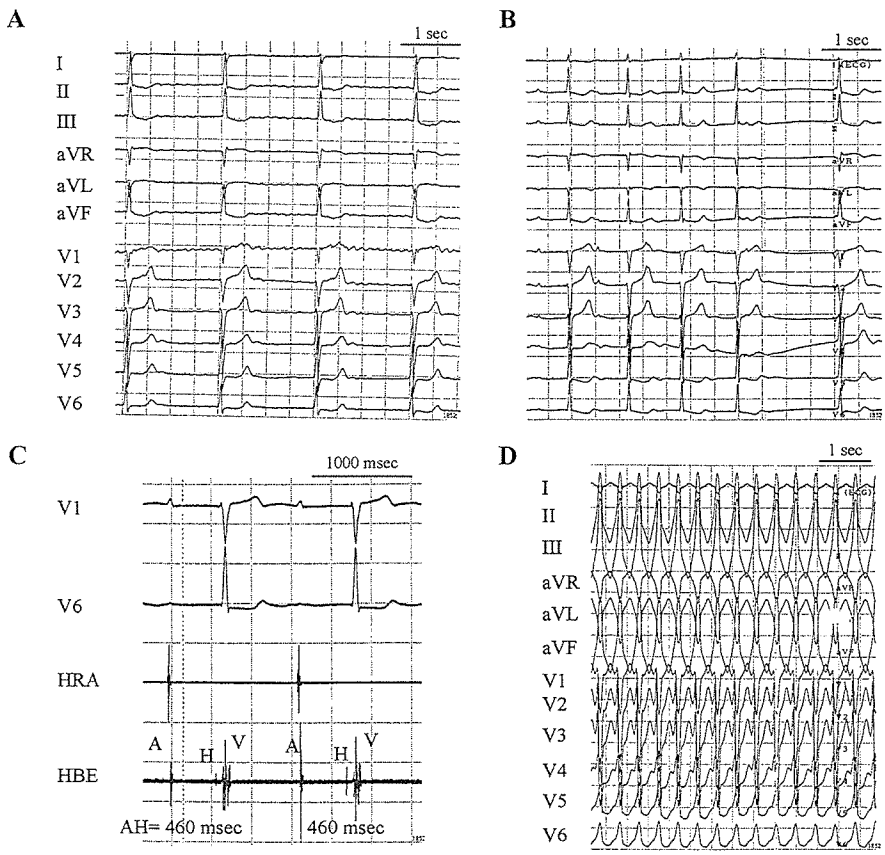

Figure 3. *Twelve-lead ECGs and intracardiac electrogram. Cardiograms were recorded during the electrophysiological study of affected member, V-65. At the beginning of the electrophysiological study, (A) AF with complicated third-degree AV block (30 ventricular beats/min) was found. (B) After a direct current defibrillation, the sinus rhythm appeared in association with Wenckebach-type second-degree AV block. (C) In the intracardiac electrogram a prolonged AH interval (460 ms) was detected during the sinus rhythm. (D) Sustained VT could be induced by programmed stimulations at the out-flow tract of the RV. HRA and HBE indicate high right atrium and His bundle electrogram, respectively.*

Table 1. Characteristics of the study subjects

Characteristic	Morning (n = 1275)	Evening (n = 1133)
Age (y)*	61.7 ± 11.8	62.1 ± 11.7
Gender (men %)	41	38
Home HR (beats/min)*	66.1 ± 7.9	68.7 ± 7.8
Home SBP (mm Hg)*	123.3 ± 15.0	120.9 ± 14.6
Antihypertensive medication (%)	29	29
BMI (kg/m^2)*	23.6 ± 3.1	23.5 ± 3.1
Time spent walking (≥1 h/day %)	79	80
Smoking status (current smoker %)	20	18
Alcohol-drinking status (current drinker %)	40	38
Coffee intake (≥1 cup/week %)	76	75
History (%)		
Stroke	3	3
Diabetes mellitus	12	12
Hypercholesterolemia	13	14

BMI = body mass index; HR = heart rate; SBP = systolic blood pressure.
* Mean ± standard deviation.

Questionnaire Survey

Information on age, antihypertensive medication, smoking and alcohol drinking status, body mass index (BMI), activity levels (time spent walking per day), coffee intake, and any history of stroke, diabetes mellitus, or hypercholesterolemia was obtained from a questionnaire sent to each subject at the time of the first home HR and BP measurement. The information on antihypertensive medication was confirmed from medical records kept at Ohasama Hospital.

Statistical Analysis

All data are expressed as mean ± SD. Variables were compared using the Pearson regression analysis, Student t test, χ^2 test, multiple linear regression analysis, or analysis of variance (ANOVA) as appropriate. The threshold level for statistical significance was set at $P < .05$. All statistical analyses were performed using SAS software, version 8.2 (SAS Institute, Cary, NC).

Results

Characteristics of the Study Subjects

Of the 1275 study subjects, 1133 (89%) measured their home HR and BP in both the morning and evening. Table 1 shows the characteristics of the study subjects who measured HR in the morning (n = 1275) and in the evening (n = 1133). The mean number of home HR measurements was 22.6 ± 6.5 for the morning and 22.8 ± 6.5 for the evening.

Of the 1275 subjects who measured HR in the morning, 365 (29%) were receiving antihypertensive medication. Of these, 232 (64%) were taking calcium (Ca) antagonists, 63 (17%) angiotensin-converting enzyme (ACE) inhibitors, 45 (12%) β-blockers, 34 (9%) α_1-blockers, 20 (5%) diuretics, 7 (2%) αβ-blockers, and 5 (1%) other drugs, respectively. The most common combinations of antihypertensive agents were Ca antagonists + ACE inhibitors (n = 46, 13%) and Ca antagonists + β-blockers (n = 40, 11%).

The characteristics of the subjects who measured HR in the evening were similar to those of the individuals who took measurements in the morning (Table 1).

Bivariate Analysis of Factors Affecting Home HR

An initial bivariate analysis was performed to determine which factors influenced home HR values. The factors investigated were age, gender, SBP, the use of antihypertensive medication, BMI, time spent walking, smoking, and alcohol-drinking status, coffee intake, and any history of stroke, diabetes mellitus or hypercholesterolemia (Table 2). Morning home HR levels showed significant negative correlation with age (r = −0.11, $P < .001$) and morning home SBP (r = −0.06, P = .02). There was also significant negative correlation between single home HR and home SBP in the morning obtained on the first day of the home measurement (r = −0.07 P = .014). There were significant differences in home HR values between subjects who were and were not taking antihypertensive medication (with antihypertensive medication, 65.3 ± 8.5 beats/min; without antihypertensive medication, 66.5 ± 7.8 beats/min, P = .01), between those who spent ≥1 h/day walking (≥1 h/day) and those who spent <h/day walking (<1 h/day) (≥1 h/day, 65.7 ± 7.9 beats/min; <1 h/day, 67.8 ± 7.8 beats/min, $P < .001$), and between current smokers and former or never smokers (current smokers, 67.8 ± 8.3 beats/min; former or never smokers, 65.8 ± 7.9 beats/min, $P < .001$). Similarly, evening home HR levels were associated with age, use of antihypertensive medication, time spent walking, and smoking. In addition, evening home HR levels were significantly as-

Table 2. Bivariate analysis of factors affecting home heart rate value

Continuous variable	Morning		Evening	
	Correlation coefficient	*P* value	Correlation coefficient	*P* value
Age	−0.11	<.001	−0.15	<.001
Home SBP	−0.06	.02	−0.01	.75
BMI	−0.02	.39	0.05	.07

Categorical variable*		Morning		Evening	
		Mean value (beats/min)	*P* value	Mean value (beats/min)	*P* value
Gender	Men	65.8 ± 8.6	.20	69.1 ± 8.5	.07
	Women	66.4 ± 7.5		68.3 ± 7.4	
Antihypertensive medication	Present	65.3 ± 8.5	.01	67.2 ± 8.2	<.001
	Absent	66.5 ± 7.8		69.2 ± 7.6	
Time spent walking	≥ 1 h/day	65.7 ± 7.9	<.001	68.4 ± 7.9	.01
	< 1 h/day	67.8 ± 7.8		70.0 ± 7.5	
Smoking	Current smoker	67.8 ± 8.3	<.001	71.0 ± 8.1	<.001
	Former or never smoker	65.8 ± 7.9		68.1 ± 7.7	
Alcohol-drinking	Current drinker	66.4 ± 8.1	.31	69.6 ± 7.8	.001
	Former or never drinker	66.0 ± 8.0		68.1 ± 7.8	
Coffee-drinking	≥ 1 cup/week	66.5 ± 8.0	.19	69.1 ± 7.8	.14
	< 1 cup/week	65.8 ± 7.9		68.3 ± 8.1	
Stroke	Present	64.9 ± 10.2	.39	67.2 ± 9.6	.33
	Absent	66.3 ± 7.9		68.8 ± 7.7	
Diabetes mellitus	Present	66.7 ± 8.7	.43	69.2 ± 8.3	.44
	Absent	66.1 ± 7.7		68.6 ± 7.5	
Hypercholesterolemia	Present	66.4 ± 8.4	.93	68.8 ± 7.8	.86
	Absent	66.3 ± 7.9		68.7 ± 7.7	

Abbreviations as in Table 1.
Continuous variables were tested by Pearson's regression analysis. Categorical variables were tested by Student *t* test.
* Mean ± standard deviation.

sociated with alcohol drinking status (current drinkers, 69.6 ± 7.8 beats/min; former or never drinkers, 68.1 ± 7.8 beats/min, $P = .001$). The other variables were not significantly associated with home HR levels.

Multivariate Linear Regression Analysis of Factors Affecting Home HR

Because many of the previously mentioned factors might be interrelated, we performed a multivariate linear regression analysis including gender and the other factors that were significantly associated with home HR levels in the bivariate analysis. The results of this analysis are summarized in Table 3. When all subjects were included, the multivariate linear regression analysis revealed significant negative relation between morning home HR and age, time spent walking, male gender, and former smoking or never smoking status. Evening home HR was significantly associated with similar variables as the morning HR other than gender. No significant associations were observed between home HR levels and the other variables including home SBP. The associations between home HR and age and smoking status were greater in men than in women. Subjects who were not taking antihypertensive medication (untreated subjects) had similar morning and evening results with the overall study population.

Effects of Antihypertensive Medication on Home HR

Multiple linear regression analysis adjusted for age, time spent walking, gender, and smoking status showed a significant inverse association between the use of β-blocker and morning home HR (Model 1, Table 4). Similarly, the use of Ca antagonist and β-blocker were significantly and inversely associated with evening home HR, whereas diuretic use was positively associated with the evening home HR (Model 1, Table 4). Because these antihypertensive drugs were simultaneously used in some cases, we included all of these drugs simultaneously in a multivariate model (Model 2, Table 4). The model showed that β-blocker inversely and independently associated with both morning and evening home HR, whereas diuretic use was positively and independently associated with evening home HR values. In addition, even when we used each type of antihypertensive medication as a covariate, results that smoking and sedentary lifestyle effects home HR value were unchanged (data not shown).

Table 3. Multivariate regression analysis of factors affecting home heart rate value

Morning	All subjects (n = 1275)		Men (n = 523)		Women (n = 752)		Untreated subjects (n = 910)	
Variable	Coefficient	*P* value	Coefficient	*P* value	Coefficient	*P* value	Coefficient	*P* value
Age (per 1 year)	−0.08	<0.001	−0.15	<.001	−0.02	.48	−0.09	<.001
Smoking (current = 1)	3.22	<0.001	3.01	<.001	2.63	.15	3.08	<.001
Time spent walking (≥1 h/day = 1)	−2.43	<0.001	−2.21	.01	−2.41	<.001	−2.06	.001
Gender (men = 1)	−2.07	<0.001	NA	NA	NA	NA	−1.90	.002
Antihypertensive medication (present = 1)	−0.32	0.57	−0.48	0.59	−0.26	0.72	NA	NA
Home SBP (per 1 mm Hg)	−0.005	0.80	0.04	0.22	−0.04	0.09	−0.003	0.88
R^2	0.052		0.095		0.025		0.050	
Evening	**All subjects (n = 1133)**		**Men (n = 432)**		**Women (n = 701)**		**Untreated subjects (n = 809)**	
Variable	**Coefficient**	***P* value**	**Coefficient**	***P* value**	**Coefficient**	***P* value**	**Coefficient**	***P* value**
Age (per 1 year)	−0.07	.002	−0.18	<.001	0.003	.91	−0.08	.001
Smoking (current = 1)	3.09	<.001	2.77	<.001	0.96	.63	2.86	<.001
Time spent walking (≥1 h/day = 1)	−1.93	<.001	−1.56	.09	−1.65	.02	−1.44	.03
Gender (men = 1)	−0.91	.14	NA	NA	NA	NA	−0.18	.80
Antihypertensive medication (present = 1)	−1.04	.06	−1.23	.17	−1.24	.07	NA	NA
Alcohol-drinking (current = 1)	0.93	.10	1.48	.09	0.61	.42	0.61	.34
R^2	0.055		0.140		0.013		0.051	

NA = not analyzed; SBP = systolic blood pressure.

Table 4. Effect of each antihypertensive drugs on home heart rate (HR) value

	Morning HR (N = 1275)				Evening HR (N = 1133)			
	Model 1		Model 2		Model 1		Model 2	
	Coefficient	P value	Coefficient	P value	Coefficient	P value	Coefficient	P value
Ca antagonist (present = 1)	−0.34	.57	0.05	.94	−1.60	.01	−1.26	.07
ACE inhibitors (present = 1)	1.47	.15	1.58	.15	0.41	.71	0.97	.40
β-Blocker* (present = 1)	−2.50	.02	−2.64	.03	−3.23	.01	−2.60	.04
α-Blocker (present = 1)	−2.18	.11	−2.19	.12	−2.74	.07	−2.18	.17
Diuretics (present = 1)	2.67	.13	2.51	.17	3.69	.04	4.07	.03

ACE = angiotensin converting enzyme; Ca = calcium.
Model 1: adjusted for age, smoking status, time spent walking, gender. Model 2: Model 1 + each antihypertensive drug.
* Including $\alpha\beta$-blockers.

Effects of Casual HR and Casual BP on Home HR

Among the 890 individuals who underwent casual HR and BP measurements, casual HR and morning home HR showed significant correlation with casual SBP and home morning SBP, respectively (casual, $r = 0.08$ $P = .02$; home, $r = -0.09$, $P = .01$). This association persisted after adjustment for major confounding factors in casual measurements ($P = .003$), although it disappeared in home measurements ($P = .3$). The difference between casual and morning home HR (casual HR value − morning home HR value) was significantly and positively associated with the difference between casual and morning home SBP ($r = 0.11$, $P = .001$). Similar results were obtained even when the correlations were calculated by using data from single home measurement obtained on the first day. Correlation between casual and morning home HR was statistically significant ($r = 0.40$, $P \leq .0001$) although it was weaker than the correlation between morning home and casual BP values (SBP: $r = 0.52$, $P \leq .0001$; DBP: $r = 0.43$, $P \leq .0001$). Similar associations were observed for evening home HR (data not shown).

Discussion

We recently clarified the strong predictive value of resting HR for CVD mortality using home HR obtained by a self-monitored blood pressure measuring device,[8] which makes it possible to obtain reliable HR values at rest through multiple measurements under stable conditions. Knowledge of the factors that affect home HR values may be useful in the reduction of risk for CVD. However, no information on the determinants of elevated home HR values has been published. Therefore, we conducted a cross-sectional community survey to identify factors that might affect home HR.

In the present study, we first identified the factors that affect home-measured resting HR in the general population. Elevated home HR was found to be associated with younger age, current smoking, walking for <1 h/day, and female gender. Among these factors influencing home HR values, smoking status, and time spent walking were modifiable. Joint effects of modification of these two were correspond to approximately 5 beats/min, suggesting that these modification may lead to a 17% decrease in CVD mortality risk.[8] However, possibility of selection bias needs to be considered to generalize the present findings, as there were differences in age or systolic BP between the study subjects and those excluded.

The gender difference in HR (higher HR in women than in men) has already been reported in several studies.[17–21] A number of studies have also reported a negative association between HR and age,[18,20,22] whereas others have shown no association between alcohol consumption and HR.[17,19,22] A negative association between HR and physical activity has also been established by some au-

HUMAN MUTATION 26(4), 285–290, 2005

MUTATION UPDATE

Mutations in the Holocarboxylase Synthetase Gene *HLCS*

Yoichi Suzuki,* Xue Yang, Yoko Aoki, Shigeo Kure, and Yoichi Matsubara

Department of Medical Genetics, Tohoku University School of Medicine, Sendai, Japan

Communicated by Mark H. Paalman

Holocarboxylase synthetase (HLCS) deficiency is an autosomal recessive disorder. HLCS is an enzyme that catalyzes biotin incorporation into carboxylases and histones. Since the first report of the cDNA sequence, 30 mutations in the *HLCS* gene have been reported. Mutations occur throughout the entire coding region except exons 6 and 10. The types of mutations are one single amino acid deletion, five single nucleotide insertions/deletions, 22 missense mutations, and two nonsense mutations. The only intronic mutation identified thus far is c.1519+5G>A (also designated IVS10+5G>A), which causes a splice error. Several lines of evidence suggest that c.1519+5G>A is a founder mutation in Scandinavian patients. Prevalence of this mutation is about 10 times higher in the Faroe Islands than in the rest of the world. The mutations p.L237P and c.780delG are predominant only in Japanese patients. These are probably founder mutations in this population. Mutations p.R508W and p.V550M are identified in several ethic groups and accompanied with various haplotypes, suggesting that these are recurrent mutations. There is a good relationship between clinical biotin responsiveness and the residual activity of HLCS. A combination of a null mutation and a point mutation that shows less than a few percent of the normal activity results in neonatal onset. Patients who have mutant HLCS with higher residual activity develop symptom after the neonatal period and show a good clinical response to biotin therapy. Hum Mutat 26(4), 285–290, 2005.

KEY WORDS: holocarboxylase synthetase; HLCS; multiple carboxylase deficiency; biotin

INTRODUCTION

Holocarboxylase synthetase (HLCS; MIM# 609018; EC 6.3.1.10) is an enzyme that catalyzes biotin incorporation into carboxylases [Achuta Murthy and Mistry, 1972; Wolf, 2001]. In humans, four carboxylases are known to be biotinylated by HLCS. They are pyruvate carboxylase, propionyl-CoA carboxylase, and methylcrotonyl-CoA carboxylases, which are mitochondrial matrix enzymes, and acetyl-CoA carboxylase, located in both the cytosol and the mitochondrial membrane. There are two acetyl-CoA carboxylases genes. The ACACA gene (MIM# 200350) gene encodes only a cytosolic enzyme whereas the ACACB gene (MIM# 601557) gene produces both the cytosolic and the mitochondrial enzymes [Pacheco-Alvarez et al., 2002]. Biotinylation of these carboxylases is essential for their enzymatic activities. Recently, HLCS has been thought to biotinylate histones, although the physiological significance has not been elucidated [Narang et al., 2004; Peters et al., 2002; Stanley et al., 2001].

Holocarboxylase synthetase deficiency (MIM# 253270) is an autosomal recessive disorder. It is also called (biotin-responsive) multiple carboxylase deficiency (MCD), because deficient HLCS activity results in reduced activity of multiple carboxylases. The exact incidence of this disease is not known. Our laboratory has diagnosed one or two new cases per year in Japan, where approximately 1.2 million babies are born every year. We suspect the incidence of HLCS deficiency is less than 1 in 100,000 live births per year in Japan. Most patients with HLCS deficiency manifest symptoms in the newborn to early infantile period [Narisawa et al., 1982; Wolf, 2001]. Symptoms of HLCS deficiency include metabolic acidosis, a characteristic organic aciduria, lethargy, hypotonia, convulsions, and dermatitis. Many symptoms of HLCS are also seen in biotinidase deficiency (MIM# 253260), another type of MCD. Some patients become symptomatic in the later infantile period, at the age of several months to years [Chikaoka et al., 1992; Gibson et al., 1996; Suormala et al., 1997, 1998]. All patients with HLCS deficiency reported thus far have responded to biotin administration. In some patients, however, the response was only partial as manifested by continued excretion of abnormal metabolites in the urine. Developmental abnormalities have also been reported in some cases in spite of high-dose biotin therapy [Baumgartner and Suormala, 1997; Santer et al., 2003; Suzuki et al., 1996; Wolf et al., 1981].

Received 8 October 2004; accepted revised manuscript 24 March 2005.

*Correspondence to: Yoichi Suzuki, Department of Medical Genetics, Tohoku University School of Medicine, 1-1 Seiryomachi, Aobaku, Sendai 980-8574, Japan.

Current address: Department of Public Health, Chiba University Graduate School of Medicine, 1-8-1 Inohana, Chuo-ku Chiba, 260-8670 Japan. E-mail: ysuzuki@faculty.chiba-u.jp

Grant sponsor: Grant-in-Aid for Scientific Research, Ministry of Education, Culture, Sports, Science and Technology of Japan; Grant sponsor: Ministry of Health, Labor, and Welfare of Japan.

DOI 10.1002/humu.20204

Published online in Wiley InterScience (www.interscience.wiley.com).

BIOLOGICAL RELEVANCE

Isolation of human cDNA for HLCS from the liver enabled the investigation of HLCS at the molecular level [Leon-Del-Rio et al., 1995; Suzuki et al., 1994]. The cDNA encoded 726 amino acids with in-frame stop codons lying at 5′ upstream of the first methionine. The deduced protein sequence contains a homologous region (amino acids numbers 448–701) to BirA, the biotin apo-carboxyl carrier protein ligase of *Escherichia coli*. This homologous portion of human HLCS is thought to be the putative biotin-binding region [Suzuki et al., 1994]. The importance of the domain outside the biotin-binding region of HLCS for enzymatic activity was examined in an expression study with HLCS deletion mutants. The N-terminal amino acid region up to Ile117 had much less effect on the enzymatic activity than the amino acid sequence between Ile117 and Met234 [Sakamoto et al., 1999]. The data are consistent with another experiment [Hiratsuka et al., 1998] and the observation that the mutations identified in patients so far are located after the amino acid residue Arg183 (Table 1). Multiple cDNA clones were isolated from the human lymphocyte cDNA library [Leon-Del-Rio et al., 1995]. They differed from human liver cDNA mainly at their 5′ ends. Using an exon-trapping method, another type of cDNA was isolated from the human myeloid cell line KG-1 [Ohira et al., 1997]. This cDNA has the longest 5′ upstream and 3′ downstream untranslated regions. Because the first and second methionine codons found in other types of cDNAs were skipped, this cDNA should produce only the shortest form of HLCS protein [Hiratsuka et al., 1998].

Comparisons of sequences of multiple cDNAs and the 21q22.1 genomic region determined in the human genome project [Hattori et al., 2000] has elucidated the organization of the exons and introns of the human HLCS gene [Yang et al., 2001). The HLCS gene spans approximately 240 kb and comprises 14 exons (Fig. 1). The first methionine codon is located in exon 6, and a stop codon in exon 14. Of the 14 introns, intron 9 is the longest (about 130 kb). It contains two polymorphic tetra-nucleotide repeats that are useful for determining a haplotype of the HLCS gene [Yang et al., 2000]. On the basis of results reported for several cDNA species, the HLCS gene probably generates multiple transcripts, although the physiological significance of this is not yet clear. We demonstrated at least three mRNA types with different transcription starting sites in human cultured cells [Yang et al., 2001]. Type 1 mRNA starts at exon 1. Type 2 mRNA starts at exon 3 and type 3 mRNA starts at exon 2. The variations at the 5′ end of the mRNA so far identified do not change the amino acid sequence of HLCS. Substantial variations were also present in the 3′ untranslated region (UTR) sequence of HLCS, where no consensus sequence for the polyadenylation signal was found [Yang et al., 2001].

MUTATIONS AND POLYMORPHISMS

Mutations

During the last 10 years since the first report of the cDNA sequence [Suzuki et al., 1994], 30 mutations in the HLCS gene have been reported (Table 1). The table includes novel mutations identified in four Japanese, two Faroese patients, one Danish, and one Spanish patient whose cases were not reported previously. Mutations occur throughout the entire coding region except exons 6 and 10 (Fig. 1). The types of mutations are one single amino acid deletion, five single nucleotide insertions/deletions, 22 missense mutations, and two nonsense mutations. The only intronic mutation identified was a single nucleotide mutation in intron 10, c.1519+5G>A (also designated IVS10+5G>A), that causes a splice error [Sakamoto et al., 2000]. Two mutations, L237P and 780delG, account for 50% of the Japanese mutant alleles [Yang et al., 2001], but are never found in other ethnic groups. The IVS10+5G>A mutation was found in north European countries; details of this will be discussed in the next section. The mutations R508W, V550M, G581S, D571N, and R565X were found in several ethnic groups.

Polymorphisms

The current public SNP database (dbSNP) shows three SNPs in the coding region of HLCS. We identified two other polymorphisms during the investigation of patients with HLCS deficiency and their family members (Table 1).

CLINICAL RELEVANCE

Founder Mutations

The IVS10+5G>A mutation was first identified in a Swedish patient who showed her first symptoms at the age of 8 years. The amelioration of her biochemical and clinical abnormalities after biotin treatment started was relatively slow among patients with HLCS [Holme et al., 1988]. This mutation resulted in abnormal splicing with a decreased level of normal mRNA [Sakamoto et al., 2000]. Holocarboxylase synthetase activity in the patient's fibroblasts was 4% of the normal level [Sakamoto et al., 2000]. Subsequently, a Danish patient and two patients from the Faroe Islands who are homozygous for this mutation have been reported [Yang et al., 2001]. In addition, one French patient and one German patient were reported to have IVS10+5G>A in a heterozygous form [Santer et al., 2003; Yang et al., 2001]. We further analyzed the cases of two unrelated Faroese patients and another Danish patient and found that all of the patients were homozygous for the mutation; so far, 16 alleles have been identified (Table 1). To determine the origin of the mutations, we investigated polymorphic microsatellite markers in the *HLCS* gene and determined the haplotypes of patients [Yang et al., 2000]. All IVS10+5G>A alleles were associated with the 2-3 haplotype.

Geographically, the Faroe Islands are located in the North Atlantic, north of Scotland, and west of Norway [Ewald et al., 1999]. The Faroese immigrated from Norway about 1,000 years ago. They have expanded in number from a few thousand to about 47,000 during the last two centuries. Because we have already confirmed five patients from distinct families on this island, the incidence may be estimated to be at least 1 in 10,000. This value may be 10 times higher than those of countries in the rest of the world. These observations strongly suggest that IVS10+5G>A is a founder mutation in Scandinavian patients with HLCS deficiency [Yang et al., 2001]. In a Faroese family with an HLCS-deficient child, we found an asymptomatic father who was also homozygous for this mutation. He has never shown clinical symptoms throughout his life, suggesting that there may be other asymptomatic IVS10+5G>A homozygotes.

The mutations L237P and 780delG are predominant only in Japanese patients [Aoki et al., 1995; Sakamoto et al., 1998; Yang et al., 2000, 2001]. We investigated the haplotype of these two mutations and found that both mutant alleles were exclusively associated with haplotype 2-2. This finding is consistent with the notion that L237P and 780delG are founder mutations in the Japanese population [Yang et al., 2000]. Although patients were found who were homozygous for L237P or compound heterozygous for L237P and 780delG, none were found who were homozygous for 780delG, suggesting that homozygous 780delG mutations may be lethal.

TABLE 1. List of Mutations and Polymorphisms in the *HLCS* Gene*

Exon/intron	Nucleotide change in cDNA	Effect on coding region	Number of alleles	Patient origin	References
Mutations					
Exon 7	c.548G>C	p.R183R	2	Unknown	Sakamoto et al. [1999]
Exon 7	c.647T>G	p.L216R	3	Australian	Dupuis et al. [1996]
				Maori	Morrone et al. [2002]
Exon 7	c.655_656insA	p.I219NfsX58	2	Japanese	Yang et al. [2001]
Exon 7	c.710T>C	p.L237P	9	Japanese	Aoki et al. [1995]
					Yang et al. [2001]
Exon 7	c.780delG	p.G261VfsX20	7	Japanese	Aoki et al. [1995]
					Yang et al. [2001]
Exon 8	c.998T>A	p.V333E	1	German	Suormala et al. [1997]
					Aoki et al. [1999]
Exon 8	c.1053_1054insC	p.L353AfsX7	1	Spanish	Briones et al. [1989]
					Yang et al. [2001]
Exon 8	c.1080A>C	p.R360S	2	Japanese	Yang et al. [2001]
Exon 8	c.1088T>A	p.V363D	2	Unknown	Dupuis et al. [1996]
Exon 9	c.1367A>G	p.Y456C	1	Malaysian	Yang et al. [2001]
Exon 9	c.1385C>T	p.T462I	1	Spanish	Aoki et al. [1999]
					Yang et al. [2001]
Exon 9	c.1409T>C	p.L470S	1	Japanese	Yang et al. [2001]
Intron 10	c.1519+5G>A	Splice defect (IVS10+5G>A)	16	Spanish	Holme et al. [1988]
				Danish	Sakamoto et al. [2000]
				Faroese	Yang et al. [2001]
				Swedish	This study
				French	
				German	
Exon 11	c.1522C>T	p.R508W	15	Japanese	Dupuis et al. [1996]
				Taiwanese	Sakamoto et al. [1998]
				Chinese	Yang et al. [2001]
				Iranian	Morrone et al. [2002]
				Other	Tang et al. [2003]
Exon 11	c.1533T>A	p.N511K	1	Italian	Morrone et al. [2002]
Exon 11	c.1553G>A	p.G518E	1	Unknown	Dupuis et al. [1996]
Exon 11	c.1589delT	p.L529RfsX15	1	German	Aoki et al. [1999]
Exon 11	c.1640T>G	p.V547G	1	German	Yang et al. [2001]
Exon 11	c.1648G>A	p.V550M	8	Japanese	Dupuis et al. [1996]
				African	Aoki et al. [1997]
				Other	Morrone et al. [2002]; Tang et al. [2003]
Exon 12	c.1693C>T	p.R565X	2	Japanese	Sakamoto et al. [1998]
				African	Yang et al. [2001]
					Tang et al. [2003]
Exon 12	c.1711G>A	p.D571N	3	German	Aoki et al. [1999]
				Spanish	Dupuis et al. [1996]
					This study
Exon 12	c.1741G>A	p.G581S	4	Italian	Fuchshuber et al. [1993]
				Turkish	Suormala et al. [1997]
					Morrone et al. [2002]
Exon 12	c.1744G>A	p.G582R	1	Italian	Morrone et al. [2002]
Exon 13	c.1828_1830del	p.T610del	2	Lebanese	Aoki et al. [1999]
					Touma et al. [1999]
Exon 13	c.1843G>T	p.D615Y	1	Spanish	This study
Exon 13	c.1990G>T	p.D634Y	1	German	Suormala et al. [1997]
Exon 13	c.1990G>A	p.D634N	2	Japanese	This study
				Chinese	Tang et al. [2003]
Exon 13	c.1992delC	p.R665DfsX41	1	French	Suormala et al. [1997]
Exon 13	c.1993C>T	p.R665X	1	Japanese	This study
Exon 14	c.2144A>G	p.D715G	1	Japanese	This study
Polymorphisms of the coding region					
Exon 6	c.285C>T	p.P95P			dbSNP# rs2230182
Exon 7	c.126G>T	p.E42D		Malaysian	Yang et al. [2001]
Exon 7	c.843C>T	p.S278S			Aoki et al. [1999]
					dbSNP# rs1065758
Exon 7	c.971G>A	p.R324H		Spanish	This study
Exon 8	c.1053T>C	p.N351N			dbSNP# rs1065759

*Intronic sequence of c.1519+5G>A is based on AB063285; others are based on NT_000411.4 (A of ATG is +1).

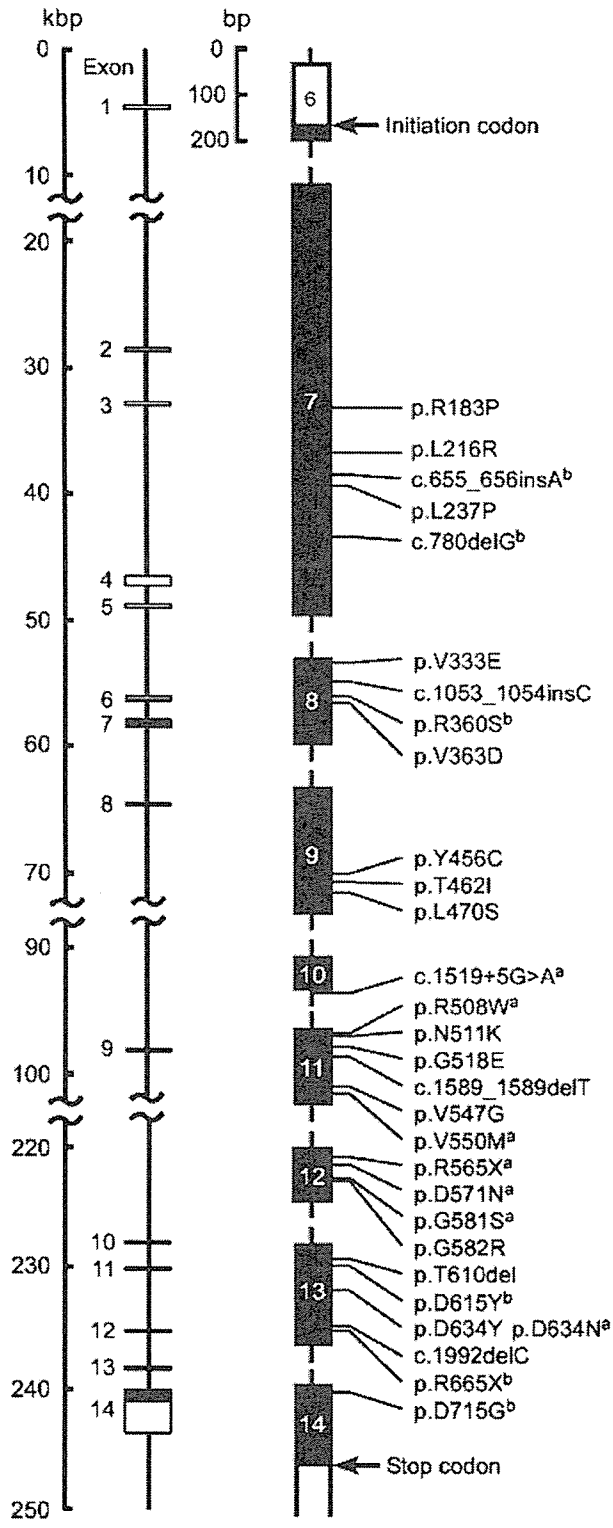

FIGURE 1. **Structure of the human holocarboxylase synthetase gene and a summary of its mutations. The *HLCS* gene spans approximately 240 kb and comprises 14 exons. The initiation codon is located in exon 6 and the stop codon is located in exon 14. Filled squares are coding exons. [a]Mutations found in several ethnic groups. [b]Mutations found in Japanese patients.**

Recurrent Mutations

The R508W mutation was found in a heterozygous form in three Japanese patients and one Chinese patient [Sakamoto et al., 1998; Tang et al., 2003; Yang et al., 2001] and in the homozygous form in three Chinese patients and one Iranian patient [Hwu et al., 2000; Morrone et al., 2002; Tang et al., 2003]. This mutation was also found in five mutant alleles in four U.S. patients whose ethnic backgrounds were not described [Dupuis et al., 1996]. The R508W mutation has been shown to have low activity in the cells [Dupuis et al., 1999]. Another mutation found in several ethnic groups is V550M. One Japanese patient was homozygous for this mutation [Aoki et al., 1997]. Dupuis et al. [1996] reported that three U.S. patients had this mutation (four alleles). Two Italian patients and one African patient were also reported to have the V550M mutation [Hwu et al., 2000; Morrone et al., 2002; Tang et al., 2003]. The mutation resulted in a decreased affinity of HLCS to biotin (i.e., a Km mutant); the mutant HLCS shows its enzymatic activity to some extent at high biotin concentrations [Aoki et al., 1997]. The R508W mutant alleles in Japanese patients were associated with either haplotype 2-3 or haplotype 1-4 [Yang et al., 2000]. The homozygous R508W mutation in the Taiwanese patient was associated with haplotype 2-3. The haplotype of the V550M mutation in the Japanese patient was 1-4, whereas that in the Jewish patient was 2-3. The nucleotide change in the R508W and the V550M mutations is a C-to-T transition at the CpG dinucleotides. These data suggest that R508W and V550M are not founder mutations but recurrent mutations occurring at CpG dinucleotide mutation hotspots [Yang et al., 2000].

Genotype–Phenotype Correlation

From an early kinetic study of mutant HLCS, patients were thought to be responsive to biotin treatment because they have mutant HLCS with a decreased affinity for biotin (i.e., a Km mutant) [Burri et al., 1985]. Using a transient expression system in HLCS-deficient fibroblasts, we further investigated the enzymatic characters of mutant enzymes [Aoki et al., 1997; Sakamoto et al., 1999]. The enzymes containing mutations that are located outside the biotin-binding region (R183P, L216R, L237P, V333E, and V363D) showed normal to higher affinity for biotin but decreased Vmax (i.e., they were non-Km mutants). The mutations located in the biotin-binding region (Gly581Ser and Thr610del) showed lower affinity for biotin (i.e., Km mutants). We usually expect that a "Km mutant" recovers its activity with high biotin concentration but a "non-Km mutant" does not. However, patients with non-Km mutants responded clinically to pharmacological doses of biotin in a manner similar to that of patients with Km mutants. The observation may be explained by our experimental data that the Km for biotin of normal HLCS is higher than the concentration of biotin in human cells under ordinary nutritional conditions [Aoki et al., 1997; Sakamoto et al., 1999].

In 16 Japanese patients from apparently unrelated families whose clinical pictures were well known, nine patients developed symptoms within a week after birth. Eight of these were compound heterozygotes of a point mutation and a null mutation (insertion/deletion and nonsense mutations). The point mutations were L237P and L470S. The null mutations were 780delG, 6556insA, and R665X. Only one patient was homozygous for L237P. We studied mutations in two European patients who displayed symptoms before they were 1 week old. One was found to be a compound heterozygote of T462I and 1053_1054insC and the other was found to be a homozygote of G581S [Yang et al., 2001].